Int J Clin Exp Pathol 2015;8(12):15759-15768
www.ijcep.com /ISSN:1936-2625/IJCEP0017759

Original Article

Role of Bcl-2 and its associated miRNAs in vasculogenic mimicry of hepatocellular carcinoma

Nan Zhao[1,2], Bao-Cun Sun[1,2,3], Xiu-Lan Zhao[1,2], Yong Wang[1], Jie Meng[1,2], Na Che[1,2], Xu-Yi Dong[1,2], Qiang Gu[1,2]

[1]Department of Pathology, Tianjin Medical University, Tianjin, China; [2]Department of Pathology, General Hospital of Tianjin Medical University, Tianjin, China; [3]Department of Pathology, Cancer Hospital of Tianjin Medical University, Tianjin, China

Received October 13, 2015; Accepted November 28, 2015; Epub December 1, 2015; Published December 15, 2015

Abstract: Objective: An investigation of the role of the anti-apoptotic protein Bcl-2 and its associated miRNAs in vasculogenic mimicry (VM) in hepatocellular carcinoma. Methods: The Bcl-2 expression plasmid was constructed for transfection into the hepatocellular carcinoma cell line HepG2. Changes in the expression profiles of the miRNAs induced by Bcl-2 overexpression and their relationships with vasculogenic mimicry were analysed. Real-time PCR was performed in frozen tissue specimens from 42 cases of hepatocellular carcinoma to analyse the relationship between Bcl-2 and miR-27a; Immunohistochemical staining was performed in paraffin-embedded tissue samples from 97 cases of hepatocellular carcinoma to analyse the relationship between Bcl-2 expression and the expression of vasculogenic mimicry (VM) related molecules VEGF and HIF1A, which were target genes of the Bcl-2 related miRNAs. Results: Overexpression of Bcl-2 results in a significant change in the expression of a wide range of miRNAs, and the target genes of these miRNAs are composed of various vasculogenic mimicry related genes; Bcl-2 expression was positively correlated with the expression of the miRNA target genes VEGF and HIF1A. The expression of VEGF and HIF1A was significantly and positively correlated with VM and poor prognosis of patients. Conclusion: Bcl-2 may play a role in vasculogenic mimicry through miRNAs by targeting angiogenesis associated genes.

Keywords: Bcl-2, miRNA, hepatocellular carcinoma, vasculogenic mimicry, VEGF, HIF1A

Introduction

MicroRNAs (miRNAs) are members of the short, non-protein coding RNA family, which are widely present in eukaryotes. They are single-stranded RNAs that consist of 19-23 nucleotides. Because they can combine with mRNA 3'-UTR and regulate the translation of gene expression at the post-transcriptional level with sequence specificity, miRNAs play an important role in biological development, fat metabolism, cell differentiation, proliferation, and apoptosis. Studies have shown that miRNAs play a key role in tumourigenesis and tumour development. They not only regulate the expression of specific blood vessel and tumour cell genes but also can directly act as oncogenes or tumour suppressors. Therefore, miRNAs have been identified as a good target for tumour classification, diagnosis, prognosis and treatment [1-4].

As a crucial regulator of apoptosis, Bcl-2 plays an important role in a variety of biological processes, such as embryogenesis and tissue homeostasis. Studies have demonstrated that the overexpression of Bcl-2 was previously related to the malignant progression of tumours [5]. Traditionally, it was believed that the oncogenic properties of Bcl-2 were related to its anti-apoptotic activity. The possible underlying mechanisms include that Bcl-2 can regulate the permeability of the mitochondrial membrane, the release apoptotic proteins, the transport of P53 across the nuclear membrane, and the glutathione redox system [6, 7]. Recent studies show that Bcl-2's role in promoting tumour cell survival may also be associated with its ability to induce tumour angiogenesis [8, 9]. In a previous study by our group, we found that Bcl-2 may play an important role in vasculogenic mimicry (VM) and metastasis in hepatocellular carcinoma [10, 11].

Some angiogenesis-related miRNAs have been previously reported. The underlying mecha-

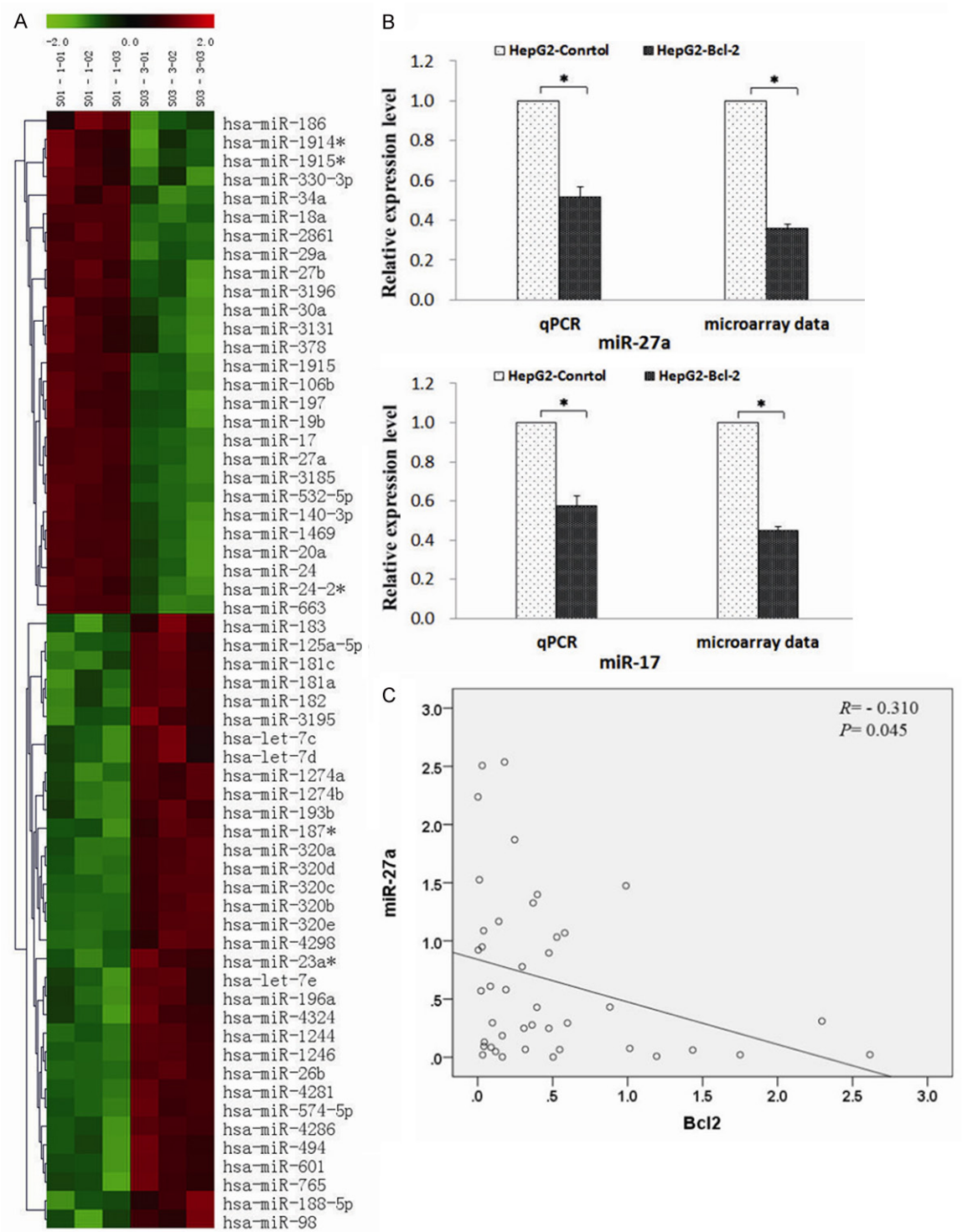

Figure 1. A. A cluster analysis (part) of differentially expressed miRNAs in HepG2-Control (left S01-1-0, 02, 03) and HepG2-Bcl-2 (right S02-2-01, 02, 03); red represents upregulation, green represents downregulation, and black represents no significant difference. B. A comparison between data from the miRNA gene microarray and real-time quantitative PCR (the miRNA expression levels in the HepG2-Control was considered to be one; the ratio of the level of corresponding miRNA expression in HepG2-Bcl-2 cells was considered to be its relative expression). C. The relationship of miR-27a and Bcl-2 in 42 cases of HCC frozen tissue specimens.

nisms and the potential target genes of these angiogenesis-related miRNAs have been studied in depth. However, it is still unclear whether Bcl-2 plays a role in VM by regulating its associ-

Table 1. List of miRNA identified in the HepG2-Control and HepG2-Bcl-2

No.	Reporter Name	*p*-value	Mean (Control)	Mean (Bcl-2)	Log2 (G2/G1)
Down-regulation					
256	hsa-miR-18a	8.87E-04	517	73	-2.83
300	hsa-miR-19b	1.70E-03	471	76	-2.63
507	hsa-miR-3185	6.18E-04	2,645	458	-2.53
388	hsa-miR-2861	1.77E-04	7,918	1,694	-2.22
321	hsa-miR-20a	9.95E-03	5,538	1,584	-1.81
31	hsa-miR-106b	7.72E-04	2,118	624	-1.76
1124	hsa-miR-663	5.75E-03	7,189	2,154	-1.74
197	hsa-miR-1469	7.80E-03	5,646	1,689	-1.74
274	hsa-miR-1915	4.70E-03	12,722	4,230	-1.59
232	hsa-miR-17	1.70E-03	4,304	1,544	-1.48
396	hsa-miR-29a	2.57E-03	4,178	1,761	-1.25
382	hsa-miR-27a	2.14E-03	9,778	4,384	-1.16
419	hsa-miR-30a	2.76E-03	3,126	1,592	-0.97
384	hsa-miR-27b	2.16E-03	4,533	2,591	-0.81
372	hsa-miR-24	8.50E-03	9,770	6,068	-0.69
519	hsa-miR-3196	9.63E-03	17,007	11,111	-0.61
Up-regulation					
518	hsa-miR-3195	4.06E-03	1,342	1,611	0.26
241	hsa-miR-182	3.71E-03	2,591	3,432	0.41
234	hsa-miR-181a	2.80E-03	609	871	0.52
529	hsa-miR-320a	6.42E-04	4,806	7,019	0.55
245	hsa-miR-183	7.41E-03	661	1,057	0.68
531	hsa-miR-320c	2.69E-04	4,045	6,802	0.75
8	hsa-let-7d	9.28E-03	10,839	18,324	0.76
6	hsa-let-7c	7.31E-03	10,469	18,175	0.8
95	hsa-miR-125a-5p	2.66E-03	968	1,711	0.82
530	hsa-miR-320b	2.05E-03	3,329	6,490	0.96
532	hsa-miR-320d	3.48E-04	2,436	5,016	1.04
533	hsa-miR-320e	2.54E-03	1,926	4,621	1.26
826	hsa-miR-4324	4.28E-03	262	693	1.41
286	hsa-miR-196a	4.11E-03	544	1,523	1.49
380	hsa-miR-26b	1.40E-03	918	2,873	1.65
10	hsa-let-7e	3.72E-03	3,636	13,029	1.84
778	hsa-miR-4281	4.39E-04	4,335	17,184	1.99
1208	hsa-miR-98	7.98E-03	365	2,630	2.85
1023	hsa-miR-574-5p	9.86E-04	114	860	2.92
783	hsa-miR-4286	7.69E-03	94	942	3.33
80	hsa-miR-1246	1.73E-04	1,160	14,413	3.64
796	hsa-miR-4298	5.75E-03	49	841	4.1

The list of miRNAs identified in the HepG2-Control and HepG2-Bcl-2 and with their mean expression values that were determined following a global normalization and a statistical analysis using student's t-test. The *P*-values for HepG2-Control vs. HepG2-Bcl-2 for each gene are <0.05.

ated miRNAs, and the mechanism of this regulation is still unclear. In this study, we analysed the miRNA expression profile changes induced by Bcl-2 upregulation and validated the relationship between Bcl-2 and target genes of miRNA in human hepatocellular carcinoma (HCC).

Results

Changes of miRNA expression profiles and Bcl-2

We assessed the miRNA expression profiles in hepatocellular carcinoma HepG2 cells and HepG2 cells transfected with plasmid pcDNA-Bcl-2. The miRNA microarray analysis showed that thousands of miRNAs had been unregulated or downregulated. Among these, 38 types of miRNA showed significant differential expression (part of the results are shown in **Figure 1A** and **Table 1**).

According to a comprehensive analysis of the target genes and related pathways, two miRNAs (miR-27a and miR-17), which may be associated with tumour angiogenesis, were selected as our main focus in the following validation study. Although there are some differences between the results of the miRNA microarray and the results of the qPCR, the basic trend was consistent (**Figure 1B**). Therefore, the authenticity of the microarray data was confirmed. The group with Bcl-2 overexpression showed that the expression of miR-27a and miR-17 was downregulated.

In addition, miR-27a was further verified in frozen human tissue specimens of HCC. Frozen tissue specimens from 42 cases of HCC were used to extract RNA, and then, the RNA was reverse transcribed to cDNA. Real-time PCR was used to detect the expression of Bcl-2 and miR-27a. A Pearson correlation analysis showed that HCC tissues with high expression of Bcl-2 were related to a decrease in the expression of miR-

Table 2. Target genes of hsa-miR-27a

Gene	Full name
CDH5	Vascular endothelium- cadherin (cadherin 5, CDH5)
XIAP	X-linked inhibitor of apoptosis protein
MAP3K14	Mitogen-activated protein kinase 14
MAPK14	Mitogen-activated protein kinase 14
PIK3CD	Phosphoinositide-3-kinase, catalytic, delta polypeptide
MAPKAPK3	Mitogen-activated protein kinase-activated protein kinase 3
EI24	Etoposide-induced protein 2.4
MDM4	Mouse double minute 4 homolog
SESN2	Sestrin-2
IGF1	Insulin-like growth factor 1
CDK6	*Cyclin-dependent kinase 6*
CCNG1	Cyclin G1
APAF1	Apoptotic protease activating factor 1
ZMAT3	Zinc finger, matrin-type 3
BBC3	BCL2 binding component 3
SP1	Specificity Protein 1
SMAD2	Drosophila mothers against decapentaplegic protein 2
VEGF	Vascular endothelial growth factor
TGFBR1	Transforming growth factor, beta receptor 1

Table 3. Target gene of hsa-miR-17

Gene	Full name
MMP2	Matrix metallopeptidase 2 (gelatinase A, 72 kDa, type IV collagenase)
VEGF-A	Vascular endothelial growth factor A
IRAK4	Interleukin-1 receptor-associated kinase 4
MAP3K14	Mitogen-activated protein kinase 14
CASP7	Caspase-7
XIAP	X-linked inhibitor of apoptosis protein
IL1RAP	Interleukin-1 receptor accessory protein
PIK3R1	Phosphatidylinositol 3-kinase, regulatory subunit, polypeptide 1
PLA2G6	Phospholipase A2, group VI
CDK6	*Cyclin-dependent kinase 6*
SESN2	Sestrin-2
CCNG2	Cyclin G2
ZMAT3	Zinc finger, matrin-type 3
TP73	Tumor protein 73
CDKN1A	Cyclin-dependent kinase inhibitor 1A
RRM2	Ribonucleotide reductase M2
TGFB1I1	Transforming growth factor beta-1-induced transcript 1
HIF1	Hypoxia inducible factor 1, alpha subunit

27a, and the difference was statistically significant (r=-0.310, P=0.04) (**Figure 1C**).

Role of miR-27a and miR-17 in angiogenesis

Determining the target genes of miRNAs through experimentation is very time consuming, and currently, there are no high-throughput methods for identifying miRNA targets. Therefore, predicting miRNA targets using theoretical methods is still the ideal technique for screening and identifying miRNA targets. TargetScan is an ideal database for predicting miRNAs using theoretical methods. The results are as follows: (1) There are 1222 types of genes that may be regulated by miR-27a. Among these genes, CDH5, SMAD2, TGFBR1, VEGF are closely related to the formation of VM (a portion of the result is shown in (**Table 2**). (2) There are 1231 types of genes that may be regulated by miR-17. Among these genes, VEGF, HIF1A, and MMP2 are closely related with the formation of VM (a portion of the result is shown in **Table 3**).

Relationship between the Bcl-2 and MVD, VM-PAS positive cycle

Immunohistochemistry (IHC) was performed on the paraffin-embedded tissue sections of 97 cases of HCC. The positive expression of Bcl-2 was shown as yellow-brown particles mainly located in the cytoplasm of the tumour cells (cytoplasm positive expression), and some positive particles could be observed around the nucleus (nucleus positive expression) (**Figure 2A**). The microvessel density (MVD) was determined in 97 cases of HCC, and its relationship with nucleus positive expression of Bcl-2 was analysed. The results showed that

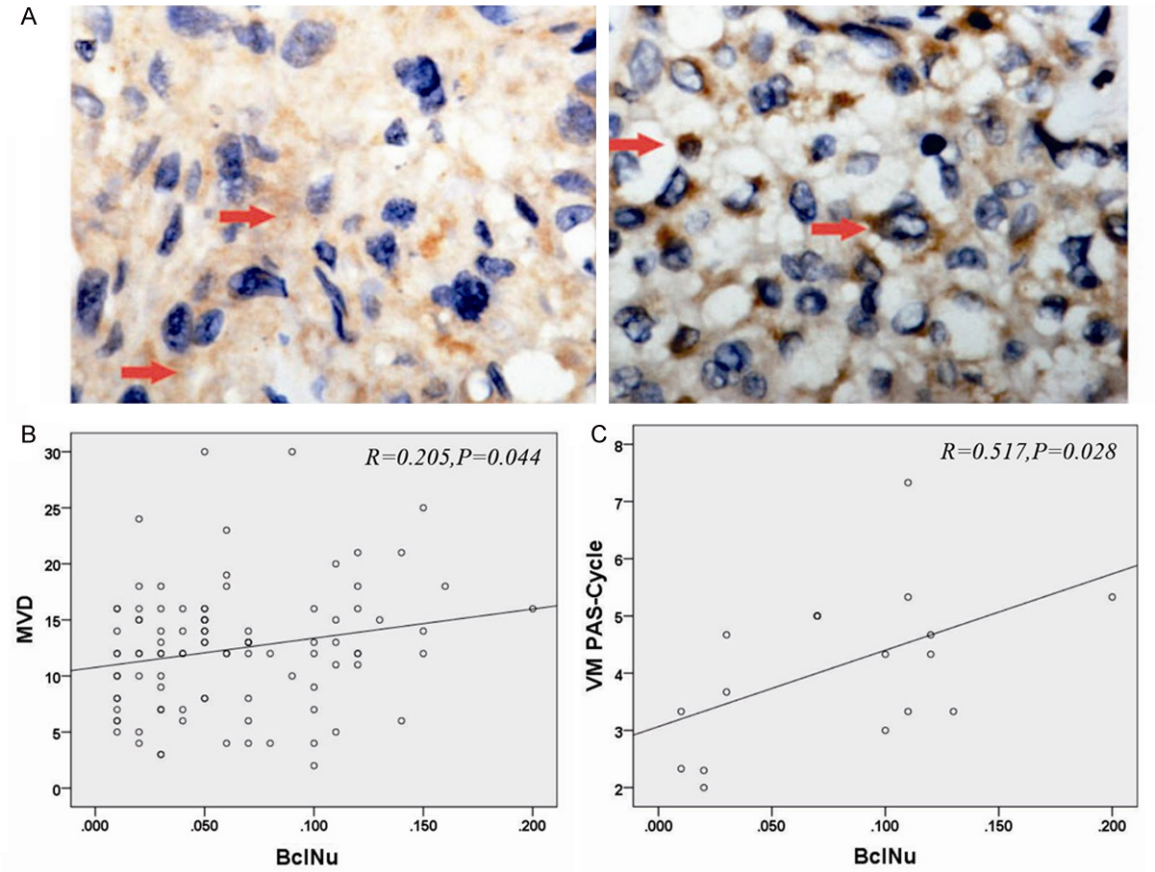

Figure 2. A. The expression of Bcl-2 in HCC tissue specimen. Left panel: expression of Bcl-2 in the cytoplasm. Right panel: expression of Bcl-2 in the nucleus, mainly expressed in the perinuclear region; B. The relationship between Bcl-2 expression and MVD; C. The relationship between Bcl-2 expression and PAS.

Bcl-2 expression was significantly and positively correlated with MVD (**Figure 2B**). VM was present in 18 cases of HCC. The VM-PAS positive cycle was counted in the VM positive tissue sections, and its relationship with nucleus positive expression of Bcl-2 was analysed as well. The results showed that Bcl-2 expression was significantly and positively correlated with the VM-PAS positive cycle (**Figure 2C**).

Relationship between expression of Bcl-2 and VEGF, HIF1A

The positive expression of VEGF presented as yellow-brown particles mainly located in the cytoplasm, and the positive expression of HIF1A presented as yellow-brown particles mainly located in the nucleus (**Figure 3**). The relationship between the nuclear expression of Bcl-2 and the expression of VEGF and HIF1A was analysed. The result showed that the nuclear expression of Bcl-2 was positively related with the positive expression of VEGF and HIF1A. The difference was statistically significant (**Figure 4**). The analysis of the relationship of VEGF and HIF1A with VM showed that VEGF and HIF1A were significantly correlated with VM ($P<0.05$) (**Table 4**). The Kaplan-Meier survival analysis was performed in 97 cases of HCC to further analyse the effect of VEGF and HIF1A on survival. The results showed that the positive expression of VEGF and HIF1A was negatively correlated with cumulative survival. The median survival time of the group with VEGF positive expression was 27 months, whereas that of the group with a lack of VEGF expression was 56 months; the median survival time of the group with HIF1A positive expression was 29 months, whereas that of the group with a lack of HIF1A expression was 42 months (**Figure 5**).

Discussion

According to their function, miRNAs can be divided into two categories: anti-angiogenic and pro-angiogenic miRNAs. Anti-angiogenic

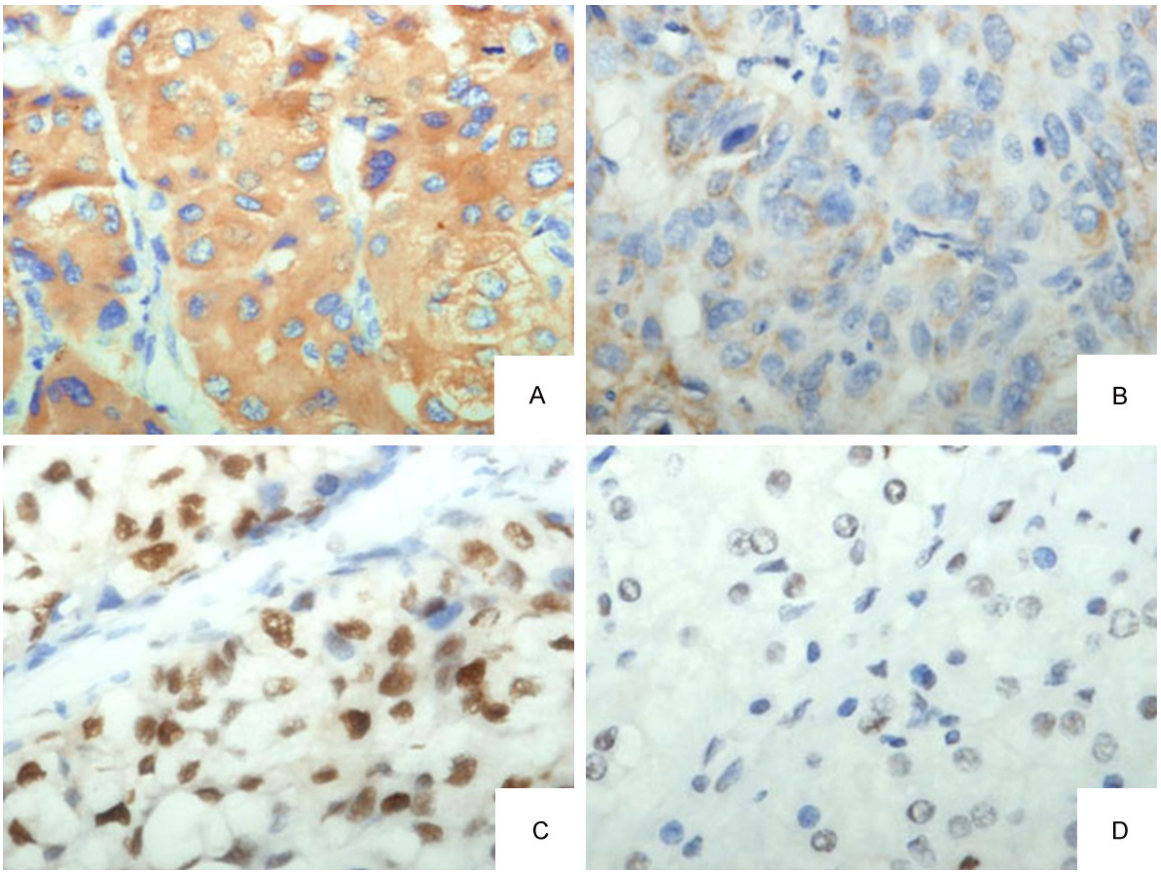

Figure 3. A. The high expression of VEGF in HCC tissue specimen. B. The low expression of VEGF in HCC tissue specimen. C. The high expression of HIF1A in HCC tissue specimen. D. The low expression of HIF1A in HCC tissue specimen (40×).

miRNAs, such as miR-7, inhibit angiogenesis in vitro and in vivo [12]; pro-angiogenic miRNAs, such as miR-145, inhibit tumour growth and angiogenesis by downregulating the expression of HIF1A and VEGF [13]. Anti-angiogenic miRNAs inhibit angiogenesis, and their expression is reduced in tumour tissue. Pro-angiogenic miRNAs induce angiogenesis, and they are often highly expressed [14]. The role of miRNAs in tumour angiogenesis is generally achieved through the regulation of cell proliferation/apoptosis, migration, adhesion and tube formation, as well as other biological processes in the multi-target approach.

In the present study, 38 types of miRNA showed significant differential expression when Bcl-2 was overexpressed. The target genes included a variety of angiogenesis related genes, including CDH5, SMAD2, TGFBR1, VEGF, HIF1A, and MMP2. VE-cadherin (CDH5) is a superfamily of transmembrane cadherin proteins that can promote cell-cell interactions. The expression of VE-cadherin is mainly located in the region of endothelial cell adherence. In addition to the regulation of cell adhesion and the maintenance of vascular permeability, VE-cadherin plays an important role in angiogenesis and the stability of the intravascular environment. Hendrix et al [15] reported VE-cadherin expression in highly invasive melanoma cells, but its expression was barely detectable in poorly invasive melanoma cells. Downregulating the expression of VE-cadherin resulted in the loss of the ability to form VM in highly invasive melanoma cells, which suggests the important role of VE-cadherin in VM formation. The high expression of VEGF was closely related with microvessel density, the degree of malignancy and a poor prognosis [16, 17]. VEGF-A belongs to the VEGF family and is the most important regulator of angiogenesis. Previous studies in our laboratory also found that the capability of ovarian cancer cells to form the vessel-like

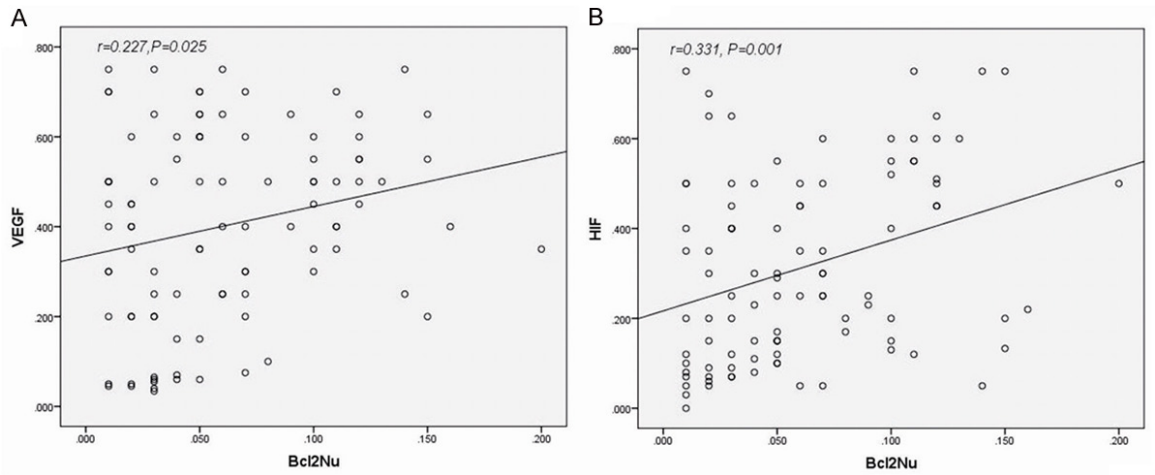

Figure 4. A. The relationship between Bcl-2 expression and VEGF expression. B. The relationship between of Bcl-2 expression and HIF1A expression.

Table 4. Relationship between VM and VEGF and HIF-1Aexpression

Variant		Tissue samples		X^2	*P*-value
		Non-VM	VM		
HIF-1A	Negative	32	2	5.564	0.018
	Positive	47	16		
VEGF	Negative	37	3	5.506	0.019
	Positive	42	15		

structure of VM in the three-dimensional culture was enhanced after adding exogenous VEGF-A in the medium. An in vitro invasion assay and wound-healing assay showed that the invasiveness and migration of ovarian cancer cells was significantly enhanced. These results confirmed that VEGF-A promoted invasion, migration and VM formation in ovarian cancer cells. The possible molecular pathway may be VEGF-a→EphA2→MMPs→VM [18]. A previous study by our group confirmed that a high expression of HIF1A was positively correlated with VM in melanoma, and its effect may be achieved by promoting the expression of VEGF [19]. Gao N also reported that HIF1A activated the expression of VEGF in tumour angiogenesis and played an important role in tumour angiogenesis and tumour progression [20].

In the present study, our results showed that the expression of miR-27a and miR-17 was reduced in HepG2 cells that overexpressed Bcl-2. Because miRNA negatively regulates the expression of its target genes, the downregulation of miR-27a and miR-17 may result in the high expression of their target genes, including VE-cadherin, MMP2, HIF1A and VEGF-A, which can induce formation of VM. The results from the human HCC specimens also confirmed that expression of Bcl-2 was positively correlated with VEGF and HIF1A, which are target genes of miR-27a and miR-17, and the positive expression of VEGF and HIF1A was positively related with the poor prognosis of patients.

In summary, the results of the present study suggest that Bcl-2 may regulate the expression of miRNA through a variety of mechanisms. This regulation may reduce the expression of miR-27a and miR-17 and weaken the miRNA-induced inhibition of target genes. Furthermore, the expression of tumour angiogenesis related genes, such as VE-cadherin, MMP2, HIF1A and VEGF-A, was enhanced. Ultimately, these changes promote the formation of VM and may affect the prognosis of patients. Further study of Bcl-2 in tumour angiogenesis may provide a new target for clinical anti-tumour therapy.

Materials and methods

Plasmid

The pcDNA3-Bcl-2 plasmids were obtained by cDNA-library subcloning and were verified by sequencing.

Cell culture and transfection

The HepG2 cell line was cultured in Dulbecco's modified Eagle's medium (HyClone) supplemented with 10% foetal bovine serum (FBS, HyClone). The plasmid vectors were transfect-

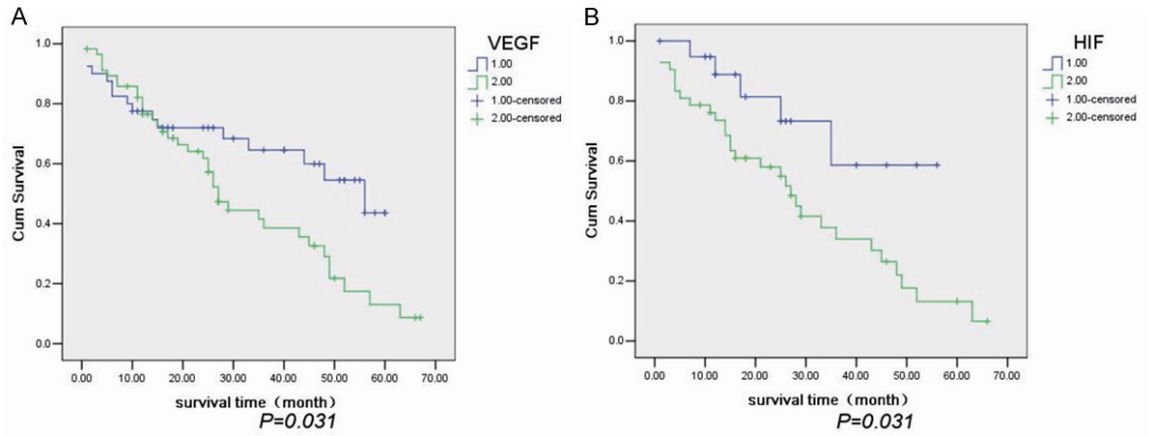

Figure 5. A. The relationship between VEGF expression and cumulative survival. B. The relationship between HIF1A expression and cumulative survival.

ed into the cells with polyethylenimine (PEI) (PolyScience, Inc., Cat#23966).

miRNA microarray analysis

HepG2-Control and HepG2-Bcl-2 cells were used. The miRNA microarray was a double channel fluorescence chip; all of the oligonucleotide probes were labelled with Cy3 (green colour) and Cy5 (red colour) fluorescent dyes. The fluorescence scanning used a double-channel laser scanner. Then, the figure signal was transformed to a digital signal using image analysis software (LuxScan 3.0, CapitalBio, Beijing, China).

Quantitative reverse transcription (RT)-PCR

The cDNA was synthesized from 2 μg of total RNA using Quant reverse transcriptase (Tiangen, China). The RT reactions were performed for 1 h at 37°C. Quantitative Reverse PCR was conducted in an ABI 7500 Real-Time PCR System (Applied Biosystems, Foster City, CA). The fluorescence intensity of the amplified products was measured at the end of each PCR cycle. Two runs were performed for each data point run in triplicate. The results were normalized to the internal control: GAPDH mRNA.

Western blot

The samples were transferred to polyvinylidene difluoride membranes (PVDF, Millipore). The blots were blocked with 5% non-fat milk for 1 h at room temperature and then incubated with the primary antibody for 1 h at room temperature with agitation. The blots were then incubated with horseradish peroxidase-conjugated secondary antibodies (1:2000; Santa Cruz). The blots were developed using an enhanced chemiluminescence detection kit (ECL; Amersham Pharmacia Biotech, Piscataway, NJ). We used rabbit polyclonal β-actin antibodies (sc1616-R, 1:200; Santa Cruz) for protein loading analyses. The intensity of the protein bands was determined by densitometry using a Gene Genius Super System (Gene Company Limited, EN).

Tissue collection

Ninety-seven HCC paraffin-embedded tissue samples, surgically resected from January 2001 to December 2005, and forty-two HCC frozen tissue specimens, surgically resected from January 2014 to December 2015, were obtained from the Tumor Tissue Bank of Tianjin Cancer Hospital. The diagnosis of HCC was verified by pathologists. The use of these tissues was approved by the Institutional Research Committee.

Immunohistochemical staining

Prior to immunostaining, 4-μm paraffin sections were deparaffinized in xylene and rehydrated by a graded series of aqueous ethanol solutions. The endogenous peroxidase activity was blocked with 3% hydrogen peroxide in 100% methanol for 15 minutes at room temperature. The sections were washed with phosphate-buffered saline (PBS) and then pre-treated with citrate buffer (0.01 mol/L citric acid, pH

6.0) for 20 minutes at 95°C in a microwave oven to expose the antigens. After the nonspecific binding sites were blocked by incubation in 10% normal goat serum in PBS for 20 minutes at 37°C, the sections were incubated overnight at 4°C with the primary antibodies. The next day, the sections were incubated with a compatible horseradish peroxidase (HRP)-conjugated secondary antibody for 30 minutes at 37°C, followed by the chromogen 3,3'-diaminobenzidine for 5 to 10 minutes at room temperature. Finally, the sections were lightly counterstained with haematoxylin for 1 minute, followed by dehydration and mounting on the coverslips. For the negative controls, PBS was used instead of the primary antibodies. The staining systems used in this study were PicTure PV6000 and Elivision Plus (Zhongshan Chemical Co, Beijing, China).

Immunohistochemical scoring

The evaluation of sections was performed by two independent pathologists that were blinded to the clinical information. The expression of each marker was semi-quantitatively assessed according to both the extension of the stained cells and the intensity of the immunostaining in the individual tumour cells [21, 22]. More than 10 microscopic fields in each section were counted with approximately 100 tumour cells per field under light microscopy. The extent of positivity ("extent of distribution" of positive cells) was graded on the following scale: 0 for less than 10% positive cells, 1 for less than 25% positive cells, 2 for less than 50% positive cells, and 3 for more than 50% positive cells. The intensity of staining was scored on a scale of 0 to 3 as follows: 0, no appreciable staining in the tumour cells; 1. barely detectable staining in the cytoplasm and/or nucleus compared to the stromal elements; 2. readily visible brown staining; and 3. dark brown staining in the tumour cells obscuring the cytoplasm and/or nucleus. The minimum score when summed (extension + intensity) was 0, and the maximum score was 6. For statistical analysis, a total score of 0 to 2 were considered negative/low expression, whereas scores of 3 to 6 were considered positive/high expression.

Microvessel density quantification

To identify the hotspots containing the greatest number of stained vessels, a vascularity assessment was performed by first scanning the section at a low power (×40) using a light microscope. For manual counts, 5 non-overlapping fields in each section were considered to acquire the MVD. In each section, 5 areas with the highest vascularization were selected [23].

Statistical analysis

All of the data were evaluated using SPSS 13.5 (SPSS Inc., Chicago, USA). The differences were considered significant at $P<0.05$. The significant groups are marked with an asterisk in the figures.

Acknowledgements

This study was funded by the Key Project of the National Nature Science Foundation of China (No. 81230050), Project of National Nature Science Foundation of China (No. 81301813, 81172046, 81173091), the Tianjin Natural Science Foundation (14JCYBJC27700), and the Natural Science Foundation of Tianjin Education Commission (20120103).

Disclosure of conflict of interest

None.

Address correspondence to: Dr. Bao-Cun Sun, Department of Pathology of Tianjin Medical University, Tianjin 300070, RP China. Tel: +86 136-02111192; Fax: 0086-22-83336813; E-mail: baocunsun@aliyun.com

References

[1] Cui SY, Wang R, Chen LB. MicroRNA-145: a potent tumour suppressor that regulates multiple cellular pathways. J Cell Mol Med 2014; 18: 1913-26.

[2] Lu J, Getz G, Miska EA, Alvarez-Saavedra E, Lamb J, Peck D, Sweet-Cordero A, Ebert BL, Mak RH, Ferrando AA, Downing JR, Jacks T, Horvitz HR Golub TR. MicroRNA expression profiles classify human cancers. Nature 2005; 435: 834-8.

[3] Zaravinos A. The regulatory role of micrornas in emt and cancer. J Oncol 2015; 2015: 865816.

[4] Zhang S, Lu Z, Unruh AK, Ivan C, Baggerly KA, Calin GA, Li Z, Bast RC Jr, Le XF. Clinically Relevant microRNAs in Ovarian Cancer. Mol Cancer Res 2015; 13: 393-401.

[5] Correia C, Lee SH, Meng XW, Vincelette ND, Knorr KL, Ding H, Nowakowski GS, Dai H, Kaufmann SH. Emerging understanding of Bcl-2 biology: Implications for neoplastic progression and treatment. Biochim Biophys Acta 2015; 1853: 1658-71.

[6] Mora N, Markovic J, De la Concepcion N, et al. Mitochondrial and nuclear relationship in apoptosis resistance. The importance of bcl-2 and redox environment. FEBS J 2010; 277: 220-21.
[7] Fulda S. Targeting apoptosis for anticancer therapy. Semin Cancer Biol 2015; 31: 84-8.
[8] Iervolino A, Trisciuoglio D, Ribatti D, Candiloro A, Biroccio A, Zupi G, Del Bufalo D. Bcl-2 overexpression in human melanoma cells increases angiogenesis through VEGF mRNA stabilization and HIF-1-mediated transcriptional activity. FASEB J 2002; 16: 1453-5.
[9] Gabellini C, De Luca T, Trisciuoglio D, Desideri M, Di Martile M, Passeri D, Candiloro A, Biffoni M, Rizzo MG, Orlandi A, Del Bufalo D. BH4 domain of bcl-2 protein is required for its proangiogenic function under hypoxic condition. Carcinogenesis 2013; 34: 2558-67.
[10] Sun T, Sun BC, Zhao XL, Zhao N, Dong XY, Che N, Yao Z, Ma YM, Gu Q, Zong WK, Liu ZY. Promotion of tumor cell metastasis and vasculogenic mimicry by way of transcription coactivation by Bcl-2 and Twist1: a study of hepatocellular carcinoma. Hepatology 2011; 54: 1690-706.
[11] Zhao N, Sun BC, Zhao XL, Liu ZY, Sun T, Qiu ZQ, Gu Q, Che N, Dong XY. Coexpression of Bcl-2 with epithelial-mesenchymal transition regulators is a prognostic indicator in hepatocellular carcinoma. Med Oncol 2012; 29: 2780-92.
[12] Babae N, Bourajjaj M, Liu Y, Van Beijnum JR, Cerisoli F, Scaria PV, Verheul M, Van Berkel MP, Pieters EH, Van Haastert RJ, Yousefi A,Mastrobattista E, Storm G, Berezikov E, Cuppen E, Woodle M, Schaapveld RQ, Prevost GP, Griffioen AW, Van Noort PI, Schiffelers RM. Systemic miRNA-7 delivery inhibits tumor angiogenesis and growth in murine xenograft glioblastoma. Oncotarget 2014; 5: 6687-700.
[13] Zou C, Xu Q, Mao F, Li D, Bian C, Liu LZ, Jiang Y, Chen X, Qi Y, Zhang X, Wang X, Sun Q, Kung HF, Lin MC, Dress A, Wardle F, Jiang BH, Lai L. MiR-145 inhibits tumor angiogenesis and growth by N-RAS and VEGF. Cell Cycle 2012; 11: 2137-45.
[14] Fasanaro P, D'Alessandra Y, Di Stefano V, Melchionna R, Romani S, Pompilio G, Capogrossi MC, Martelli F. MicroRNA-210 modulates endothelial cell response to hypoxia and inhibits the receptor tyrosine kinase ligand Ephrin-A3. J Biol Chem 2008; 283: 15878-83.
[15] Maniotis AJ, Folberg R, Hess A, Seftor EA, Gardner LM, Pe'er J, Trent JM, Meltzer PS, Hendrix MJ. Vascular channel formation by human melanoma cells in vivo and in vitro: vasculogenic mimicry. Am J Pathol 1999; 155: 739-52.
[16] Scartozzi M, Faloppi L, Svegliati Baroni G, Loretelli C, Piscaglia F, Iavarone M, Toniutto P, Fava G, De Minicis S, Mandolesi A, Bianconi M, Giampieri R, Granito A, Facchetti F, Bitetto D, Marinelli S, Venerandi L, Vavassori S, Gemini S, D'Errico A, Colombo M, Bolondi L, Bearzi I, Benedetti A, Cascinu S. VEGF and VEGFR genotyping in the prediction of clinical outcome for HCC patients receiving sorafenib: the ALICE-1 study. Int J Cancer 2014; 135: 1247-56.
[17] Anannamcharoen S and Nimmanon T. Study of the vascular endothelial growth factor (VEGF) expression and microvascular density (MVD) in primary colorectal cancer specimens. J Med Assoc Thai 2012; 95: 1041-7.
[18] Wang JY, Sun T, Zhao XL, Zhang SW, Zhang DF, Gu Q, Wang XH, Zhao N, Qie S, Sun BC. Functional significance of VEGF-a in human ovarian carcinoma: role in vasculogenic mimicry. Cancer Biol Ther 2008; 7: 758-66.
[19] Sun B, Zhang D, Zhang S, Zhang W, Guo H, Zhao X. Hypoxia influences vasculogenic mimicry channel formation and tumor invasion-related protein expression in melanoma. Cancer Lett 2007; 249: 188-97.
[20] Gao N, Ding M, Zheng JZ, Zhang Z, Leonard SS, Liu KJ, Shi X, Jiang BH. Vanadate-induced expression of hypoxia-inducible factor 1 alpha and vascular endothelial growth factor through phosphatidylinositol 3-kinase/Akt pathway and reactive oxygen species. J Biol Chem 2002; 277: 31963-71.
[21] Rahman MA, Dhar DK, Yamaguchi E, Maruyama S, Sato T, Hayashi H, Ono T, Yamanoi A, Kohno H, Nagasue N. Coexpression of inducible nitric oxide synthase and COX-2 in hepatocellular carcinoma and surrounding liver: possible involvement of COX-2 in the angiogenesis of hepatitis C virus-positive cases. Clin Cancer Res 2001; 7: 1325-32.
[22] Cheng AL, Huang WG, Chen ZC, Peng F, Zhang PF, Li MY, Li F, Li JL, Li C, Yi H, Yi B, Xiao ZQ. Identification of novel nasopharyngeal carcinoma biomarkers by laser capture microdissection and proteomic analysis. Clin Cancer Res 2008; 14: 435-45.
[23] Foote RL, Weidner N, Harris J, Hammond E, Lewis JE, Vuong T, Ang KK, Fu KK. Evaluation of tumor angiogenesis measured with microvessel density (MVD) as a prognostic indicator in nasopharyngeal carcinoma: results of RTOG 9505. Int J Radiat Oncol Biol Phys 2005; 61: 745-53.